Preprints.org

Article

Not peer-reviewed version

Interstitial N-Doped TiO2 for Photocatalytic Methylene Blue Degradation under Visible Light Irradiation

Dezheng Li , Vilanculo Clesio Calebe , Yuqiao Li , Huimin Liu * , Yiming Lei *

Posted Date: 22 August 2024

doi: 10.20944/preprints202408.1629.v1

Keywords: TiO2; nitrogen doping; photocatalytic activity; methylene bule degradation; visible light

Preprints.org is a free multidiscipline platform providing preprint service that is dedicated to making early versions of research outputs permanently available and citable. Preprints posted at Preprints.org appear in Web of Science, Crossref, Google Scholar, Scilit, Europe PMC.

Copyright: This is an open access article distributed under the Creative Commons Attribution License which permits unrestricted use, distribution, and reproduction in any medium, provided the original work is properly cited.

Preprints.org (www.preprints.org) | NOT PEER-REVIEWED | Posted: 22 August 2024 doi:10.20944/preprints202408.1629.v1

Disclaimer/Publisher's Note: The statements, opinions, and data contained in all publications are solely those of the individual author(s) and contributor(s) and not of MDPI and/or the editor(s). MDPI and/or the editor(s) disclaim responsibility for any injury to people or property resulting from any ideas, methods, instructions, or products referred to in the content.

Article

Interstitial N-Doped TiO_2 for Photocatalytic Methylene Blue Degradation under Visible Light Irradiation

Dezheng Li [1,+], Vilanculo Clesio Calebe [1,+], Yuqiao Li [1,+], Huimin Liu [1,*], and Yiming Lei [2,*]

[1] School of Chemical and Environmental Engineering, Liaoning University of Technology, Jinzhou 121001, China

[2] Departament de Química (Unitat de Química Inorgànica), Facultat de Ciències, Universitat Autònoma de Barcelona (UAB), Cerdanyola del Valles, 08193 Barcelona, Spain

* Correspondence: Huimin Liu, email: liuhuimin08@tsinghua.org.cn, Yiming Lei, email: Yiming.Lei@uab.cat

+ These authors contributed equally to the manuscript.

Abstract: Photocatalysis is a promising method for methylene blue (MB) degradation due to its effectiveness and environmental compatibility. Among photocatalysts, titanium dioxide (TiO_2) has been widely used for MB degradation due to its exceptional photocatalytic activity. However, the wide bandgap limits the degradation efficiency of TiO_2 under visible light. Herein, an interstitial nitrogen-doped TiO_2 (5%N_T/TiO_2) used thiourea as the N source is fabricated for the visible light-derived MB degradation. 5%N_T/TiO_2 exhibits an extended visible light absorption range. Besides, photoelectrochemical measurement shows an improvement in photocurrent response and charge transfer behavior on N/TiO_2. Thus, 5%N_T/TiO_2 has enhanced photocatalytic activity compared to pristine TiO_2 and substitutive N-doped TiO_2 (5%N_{AB}/TiO_2). The accelerated photocatalytic MB degradation process on N/TiO_2 should be mainly attributed to the interstitial N doping, which causes the appearance of new energy states and extended optical properties.

Keywords: TiO_2; nitrogen doping; photocatalytic activity; methylene bule degradation; visible light

1. Introduction

Methylene blue (MB) is a common dye used in various industries.[1,2] However, with its widespread utilization, MB leads to significant environmental challenges including water pollution, toxicity to aquatic life, bioaccumulation, and potential human health risks.[3,4] Thus, effective removal of MB is crucial for ecosystems and human health. Several strategies have been developed for MB remediation, such as advanced oxidation processes (AOPs), adsorption techniques, bioremediation, and membrane filtration.[5,6] Among them, based on AOPs technology, photocatalytic degradation of organic compounds is an ideal method for the removal of industrial pollutants with solar energy as the only input energy source. Improving photocatalytic degradation efficiency has been attracting a great deal of research interest.

The design of the photocatalyst is so important for photocatalytic degradation that determines the whole reaction efficiency [7–10]. Titanium dioxide (TiO_2) is a widely studied semiconductor material known for its excellent photocatalytic properties, chemical stability, and non-toxicity. It has garnered significant attention for applications in environmental remediation, particularly in the degradation of organic pollutants. However, the practical application of TiO_2 is limited by its wide bandgap (~3.2 eV for anatase), which restricts its photo-response ability to the ultraviolet light region, constituting only about 5% of the solar spectrum. In order to improve the photoconversion efficiency and photocatalytic degradation property of TiO_2, it is necessary to develop a reliable strategy for extending the photo-response range of TiO_2 photocatalyst. Nitrogen doping is a promising approach to modify the electronic structure of TiO_2 and enhance its visible light absorption capabilities[11,12]. By incorporating nitrogen atoms into the TiO_2 lattice, the bandgap can be narrowed, allowing it to

© 2024 by the author(s). Distributed under a Creative Commons CC BY license.

Preprints.org (www.preprints.org) | NOT PEER-REVIEWED | Posted: 22 August 2024 doi:10.20944/preprints202408.1629.v1

absorb visible light and thus improving its photocatalytic efficiency under solar irradiation[13–15]. Although numerous studies have proved the positive influences of N element doping in the photocatalytic activity of TiO_2, the effects of different N precursors achieving N doping should be further explored to elucidate the impact of N atoms on the structure and activity of TiO_2.

In this study, nitrogen-doped TiO_2 catalysts (denoted as $5\%N_T/TiO_2$ and $5\%N_{AB}/TiO_2$ with 5 wt% of N element content) are prepared via two different N sources (i.e. thiourea and ammonium bicarbonate) and used for photocatalytic MB degradation under visible light irradiation. A series of characterizations confirm the successful N element doping into TiO_2. When thiourea is used as the N source, N is mainly incorporated into the lattice of $5\%N_T/TiO_2$ in the form of interstitial N. On the other hand, N atoms from ammonium bicarbonate are mainly incorporated into $5\%N_{AB}/TiO_2$ in the form of oxygen substitution. Moreover, $5\%N_T/TiO_2$ possesses an improved visible light absorption capacity. The photoelectrochemical experiments indicate that the N doping increased the number of photoexcited electrons from $5\%N_T/TiO_2$ under visible light illumination. Therefore, compared to TiO_2 and $5\%N_{AB}/TiO_2$, $5\%N_T/TiO_2$ shows the optimal photocatalytic degradation performance with more than 60% of the MB removal rate within 150 min.

2. Results and Discussion

2.1. XRD Patterns of TiO_2, $5\%N_T/TiO_2$ and $5\%N_{AB}/TiO_2$ Catalysts

XRD analysis is performed to determine the crystalline phases and crystallographic structure of $5\%N_T/TiO_2$, $5\%N_T/TiO_2$ and TiO_2 catalysts (Figure1a). The undoped TiO_2 mainly consists of the rutile crystalline phase. The peaks centered at 27.5°, 36.1°, 41.3°, and 54.3° correspond to the (110), (101), (111), and (211) crystal planes of the rutile phase, respectively[16]. When TiO_2 is doped with thiourea as the nitrogen source, $5\%N_T/TiO_2$ mainly shows anatase phase. The peaks centered at 25.2°, 37.8°, 48.0°, and 55.0° correspond to the (101), (004), (200), and (211) crystal planes of the anatase phase, respectively[16]. While the $5\%N_{AB}/TiO_2$ with ammonium bicarbonate as the nitrogen source mainly shows a mixed crystal phase of rutile and anatase. Besides, the (101) crystal plane of $5\%N_T/TiO_2$ shifts from 25.2° to 26.1°. It indicates that the interstitial doping, which can cause lattice distortion, is achieved in $5\%N_T/TiO_2$. However, $5\%N_{AB}/TiO_2$ maintains two TiO_2 phases without peak shift, meaning that the doping mode of N in $5\%N_{AB}/TiO_2$ may be substitutive doping.

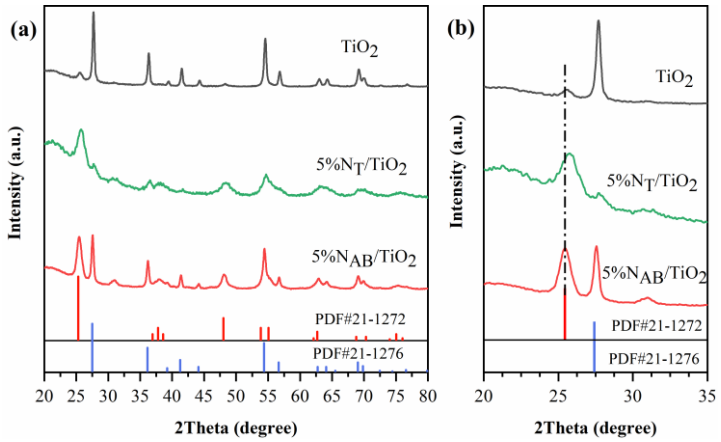

Figure 1. XRD patterns of (a) TiO_2, $5\%N_T/TiO_2$ and $5\%N_{AB}/TiO_2$, and (b)the local magnification image of XRD.

2.2. XPS Spectra of TiO_2, $5\%N_T/TiO_2$ and $5\%N_{AB}/TiO_2$ Catalysts

XPS analysis is conducted to investigate the surface elemental composition of TiO_2, $5\%N_T/TiO_2$ and $5\%N_{AB}/TiO_2$ catalysts. The results revealed that the XPS results of catalysts showed the presence of Ti 2p, O 1s, and N 1s peaks (Figure 2). The XPS spectra of $5\%N_T/TiO_2$ and $5\%N_{AB}/TiO_2$ revealed the presence of nitrogen, indicating that nitrogen was doped into TiO_2.

Preprints.org (www.preprints.org) | NOT PEER-REVIEWED | Posted: 22 August 2024 doi:10.20944/preprints202408.1629.v1

Figure 2 (a) illustrates the HR-XPS spectra of Ti 2p in TiO_2, 5%N_T/TiO_2 and 5%N_{AB}/TiO_2. For TiO_2, the Ti 2p3/2 and 2p1/2 core energy level peaks appear at 459.1 and 464.9 eV respectively, which are contributed by O-Ti-O in TiO_2[17–19]. Compared with TiO_2, in 5%N_T/TiO_2, the Ti 2p3/2 and 2p1/2 core energy level peaks appear at 458.8 and 464.5 eV, respectively, which are the Ti 2p peaks of N-Ti-N or O-Ti-N in N-TiO_2[18–20]. For 5%N_{AB}/TiO_2, the Ti 2p peaks of 5%N_{AB}/TiO_2 shift to the lower binding energy with ~ 0.4 eV changes. The peak shifts of Ti 2p indicate the successful N incorporation in both 5%N_T/TiO_2 and 5%N_{AB}/TiO_2 [17,18].

In Figure 2(b), TiO_2 exhibits the O 1s peak at 529.9 eV, which is attributed to the lattice oxygen (Ti-O-Ti). And the peak at 531.8 eV is surface-adsorbed oxygen. In 5%N_{AB}/TiO_2 and 5%N_T/TiO_2, the peaks have an obvious shift owing to the interstitial doping of N into the TiO_2 lattice to form hyponitrite ($(N_2O_2)^{2-}$, which will be further confirmed in the FTIR analyses as discussed below.

Figure 2(c) clearly shows the binding energies of N 1s at 399.8 and 401.9 eV for 5%N_T/TiO_2 and 5%N_{AB}/TiO_2, respectively. For the 5%N_T/TiO_2, according to the previous literature[21], the peak at 401.9 eV means the formation of Ti-O-N bonds based on the form of interstitial N in the lattice gap of 5%N_T/TiO_2. In the XPS spectrum of 5%N_{AB}/TiO_2 the peak of N 1s at 399.8 eV can be attributed to the Ti-N-Ti bonding, which is due to the substitution of oxygen in the 5%N_T/TiO_2 lattice by N and thus consists of the XRD results.

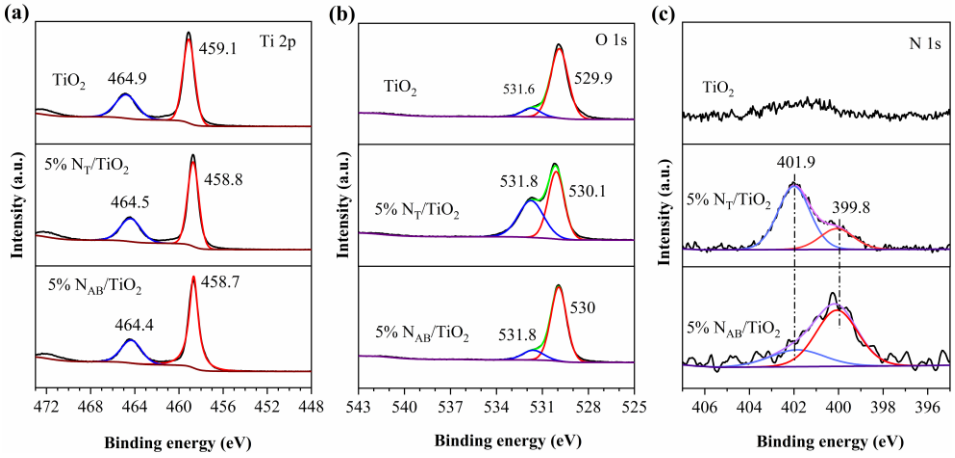

Figure 2. XPS survey spectra. (a)Ti 2p XPS spectra, (b)O 1s spectra, and (c)N 1s spectra of catalysts.

2.3. TEM Images of TiO_2, 5%N_T/TiO_2 and 5%N_{AB}/TiO_2 Catalysts

TEM characterization is used to observe the morphology of TiO_2 and N/TiO_2 catalysts. Undoped TiO_2 typically mainly shows rutile phases with particle sizes ranging from 25 to 50 nm (Figure 3a). After N element doping, the crystal phase of 5%N_T/TiO_2 transformed into the anatase phase, while 5%N_{AB}/TiO_2 mainly a mixture of rutile and anatase phases(Figure 3b and Figure 3c). The particle sizes of 5%N_T/TiO_2 and 5%N_{AB}/TiO_2 are slightly smaller than that of TiO_2. Among them, 5%N_T/TiO_2 has the smallest particle size (5.5-8 nm). HR-TEM images show clear lattice fringes with interplanar spacing of 3.20 Å and 2.48 Å (Figure 3d and Figure 3f), corresponding to the (110) and (101) facet of rutile TiO_2 respectively. The lattice spacings of 3.48 Å and 3.51 Å (Figure 3e and 3f), respectively, are corresponding to those of the (101) plane of anatase TiO_2 in 5%NT/TiO_2 and 5%N_{AB}/TiO_2. It can be observed that due to the difference in doping methods, significant differences in the lattice spacings of 5%N_T/TiO_2 and 5%N_{AB}/TiO_2 were induced. This is because 5%N_T/TiO_2 is interstitial doping, and N doping is in the lattice gap of TiO_2, which lead to lattice distortion.

Preprints.org (www.preprints.org) | NOT PEER-REVIEWED | Posted: 22 August 2024 doi:10.20944/preprints202408.1629.v1

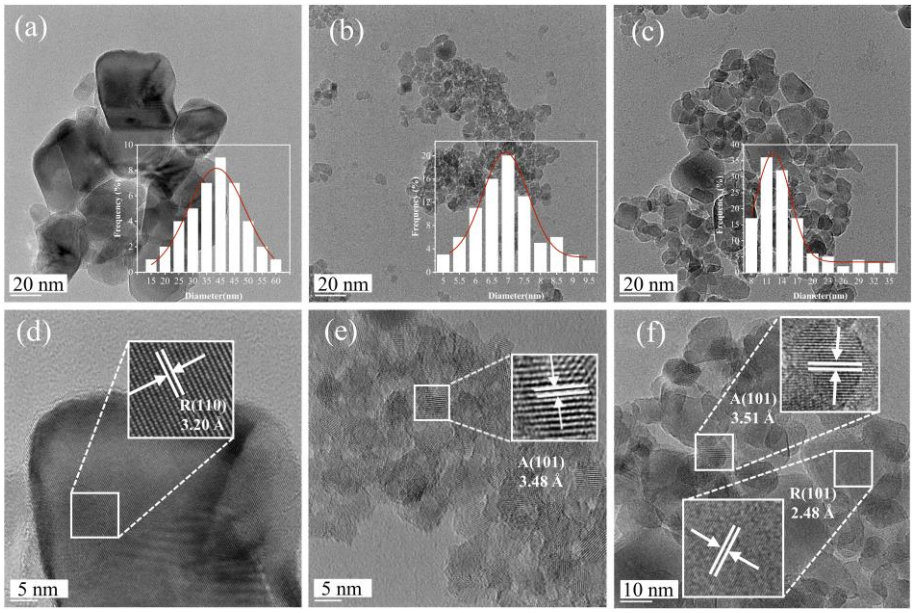

Figure 3. TEM and HRTEM images for TiO_2 (a, d), 5%N_T/TiO_2 (b, e), and 5%N_{AB}/TiO_2 (c, f). Where, R: Rutile, A: Anatase.

2.4. N_2 Adsorption-Desorption Isotherms Analysis of TiO_2, 5%N_T/TiO_2 and 5%N_{AB}/TiO_2 Catalysts

N_2 adsorption-desorption isotherms analysis is used to determine the specific surface area and porosity of TiO_2, 5%N_T/TiO_2 and 5%N_{AB}/TiO_2 catalysts. The N_2 isotherms of TiO_2, 5%N_T/TiO_2 and 5%N_{AB}/TiO_2 display IV-type isotherms (Figure 4a). It indicates that all the catalysts have mesoporous structures with 2–40 nm of pore size distributions (Figure 4b). 5%N_T/TiO_2 has a lower pore size distribution. Figure 4b and Table 1 show that the N doping, which can create additional surface defects and porosity, leads to higher specific surface area and pore size. The larger specific surface area is beneficial for mass transfer during photocatalytic reactions.

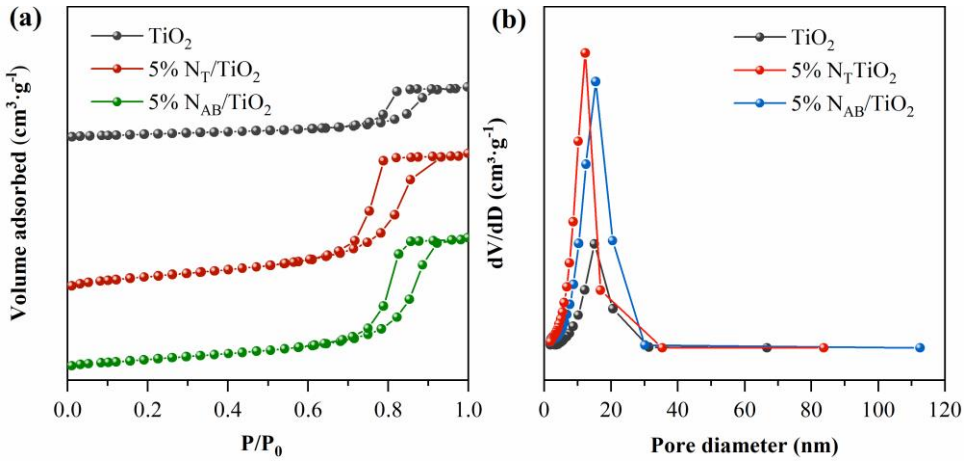

Figure 4. (a) N_2 adsorption-desorption isotherms and (b) pore size distribution of catalysts.

Table 1. BET surface area and average pore size of the catalysts.

Catalysts	Surface area ($m^2 \cdot g^{-1}$)	Average pore size (nm)
TiO_2	37.0	9.5
5%N_T/TiO_2	107.7	3.5
5%N_{AB}/TiO_2	90.0	9.6

Preprints.org (www.preprints.org) | NOT PEER-REVIEWED | Posted: 22 August 2024 doi:10.20944/preprints202408.1629.v1

2.5. FTIR of TiO_2, 5%N_T/TiO_2 and 5%N_{AB}/TiO_2. Catalysts

FTIR spectroscopy is employed to identify the presence of nitrogen-related species. (Figure 5). The characteristic peaks in the low wavenumber range (400–4000 cm^{-1}) are attributed to TiO_2. The spectra show characteristic peaks of TiO_2 at 3400 cm^{-1}, 1630 cm^{-1}, and 700–500 cm^{-1}, which are attributed to the Ti-OH bond, OH bending vibration of water molecules, and Ti-O-Ti bond stretching vibrations, respectively. The spectra of 5%N_T/TiO_2 and 5%N_{AB}/TiO_2 exhibit additional peaks at 1427–1430 cm^{-1} and 1280–1295 cm^{-1}. These peaks are attributed to the vibrations of the N-Ti bond, indicating that N atoms have been incorporated into the TiO_2 lattice. Notably, the 5%N_T/TiO_2 presents additional peaks at 1388 cm^{-1} is also attributed to the stretching vibration of N-O. Several bands in the low-frequency region observed at 1050 and 1250 cm^{-1} belong to the N^+-O type substances embedded in the TiO_2 network. The peak at 1150 cm^{-1} is the vibration peak of $(N_2O_2)^{2-}$ formed by interstitial N and O.

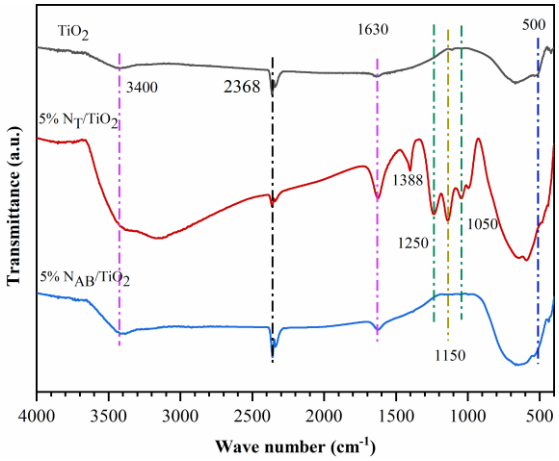

Figure 5. FTIR spectra of pure TiO_2, 5%N_T/TiO_2 and 5%N_{AB}/TiO_2 catalysts.

2.6. Optical Properties of TiO_2, 5%N_T/TiO_2 and 5%N_{AB}/TiO_2 Catalysts

The light-harvesting capacities of TiO_2, 5%N_T/TiO_2 and 5%N_{AB}/TiO_2 catalysts were evaluated via UV-vis spectroscopy as shown in Figure 6. TiO_2 showed a typical absorption edge at 420 nm, suggesting the lack of visible light response ability in TiO_2. On the contrary, N doping enhanced the visible light absorption of 5%N_T/TiO_2 and 5%N_{AB}/TiO_2. of which the light absorption edge is ~520 nm. Therefore, the incorporation of nitrogen into the TiO_2 lattice leads to the formation of new energy states, as the N 2p position is more negative than the O 2p state, leading to a decrease in the energy bandgap and a shift in the optical absorption towards the visible light region.

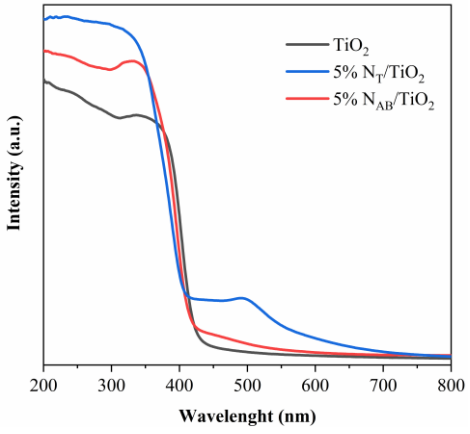

Figure 6. UV-vis spectra of TiO_2, 5%N_T/TiO_2 and 5%N_{AB}/TiO_2 catalysts.

Preprints.org (www.preprints.org) | NOT PEER-REVIEWED | Posted: 22 August 2024 doi:10.20944/preprints202408.1629.v1

2.7. Photoelectrochemical Measurements of TiO_2, 5%N_T/TiO_2 and 5%N_{AB}/TiO_2 Catalysts

The photoelectrochemical (PEC) measurement is conducted to study the photocurrent responses and charge transfer behavior (Figure 7a). TiO_2 exhibits a lower photocurrent density under visible light irradiation due to its narrow light absorption range. 5%N_T/TiO_2 and 5%N_{AB}/TiO_2 show enhanced photocurrent density under visible light, indicating nitrogen doping makes 5%N_T/TiO_2 and 5%N_{AB}/TiO_2 can convert visible light into photoexcited charges. In the electrochemical impedance spectroscopy (EIS) (Figure 7b), 5%N_T/TiO_2 and 5%N_{AB}/TiO_2 catalysts show lower semicircles compared to TiO_2, indicating lower charge transfer resistance and better charge separation. [22,23] Among them, 5%N_T/TiO_2 has the lowest resistance and the strongest photocurrent because of the smaller lattice spacing of 5%N_{AB}/TiO_2 as shown in the HR-TEM image. In general, the smaller lattice spacing means that the atoms or ions are closer to each other and electrons move more easily in the lattice, resulting in lower resistance and stronger photogenerated carriers.[24,25]

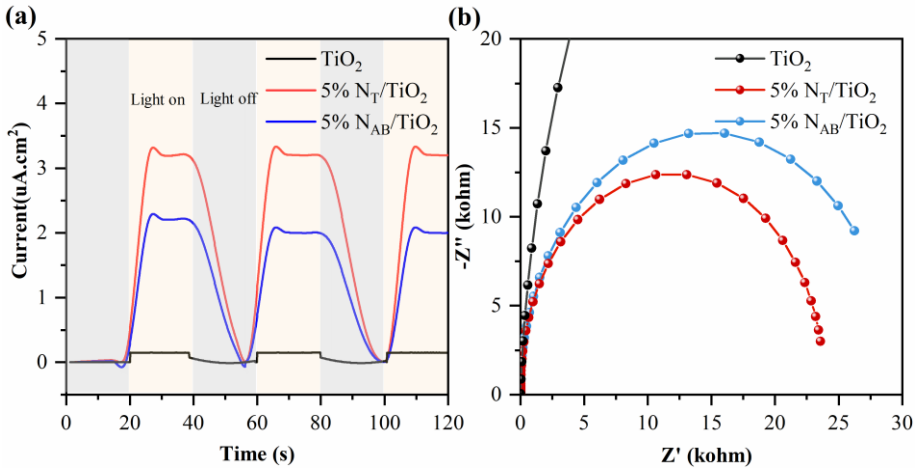

Figure 7. (a) Photoinduced i-t curves and (b) EIS curves of TiO_2, 5%N_T/TiO_2 and 5%N_{AB}/TiO_2 catalysts.

2.8. Photocatalytic MB Degradation Activity

The concentration of nitrogen doping is optimized by gradually increasing the amount of nitrogen elements in 5%N_{AB}/TiO_2 and 5%N_T/TiO_2 in terms of the degradation efficiency of MB. Figure 8 shows the efficiencies of photocatalytic MB degradation with different N doping amounts. Under visible light irradiation, undoped TiO_2 exhibits ~15 % MB degradation after 150 min (Figure 8a). For the 5%N_{AB}/TiO_2 catalysts, 5%N_T/TiO_2 has the highest MB photodegradation efficiency. After 150 min, approximately 55% of MB was degraded. The activity decline of 10%N_T/TiO_2 and 15%N_T/TiO_2 should be attributed to the excessive N atoms, which can be recombination sites of photoexcited charges as previous reports[26–28]. In addition, the above results displayed that N doping significantly enhances the catalytic performance of TiO_2 in the degradation of MB under visible light irradiation. It should be noted that the activity of 5%N_{AB}/TiO_2 is lower than that of 5%N_T/TiO_2 (Figure 8b), suggesting that interstitial doping is more effective than substitutive doping.

Preprints.org (www.preprints.org) | NOT PEER-REVIEWED | Posted: 22 August 2024 doi:10.20944/preprints202408.1629.v1

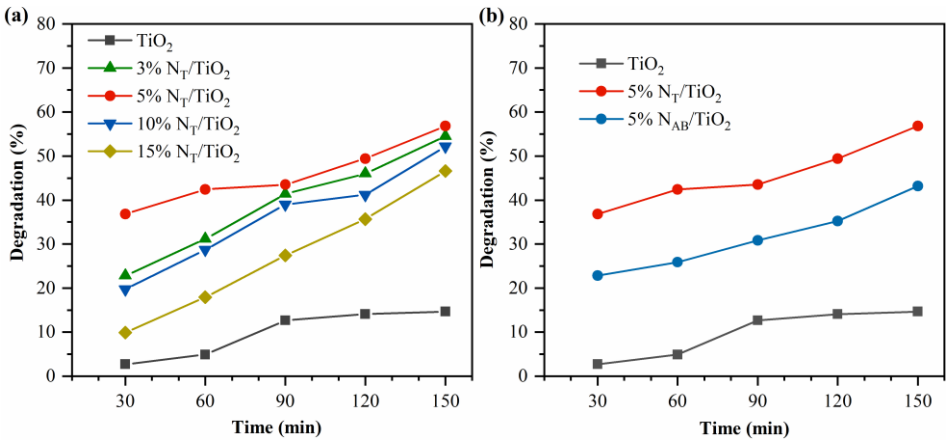

Figure 8. (a) The degradation rates of MB solution by N_T/TiO_2 photocatalysts with different N doping amounts. (b) Comparison of the degradation rates of MB by TiO_2, $5\%N_T/TiO_2$ and $5\%N_{AB}/TiO_2$ photocatalysts.

3. Materials and Methods

3.1. Catalyst Preparation

3.1.1. $5\%N_T/TiO_2$ Preparation

First, 40 min of tetrabutyl titanate was uniformly dispersed in 50 min of ethanol solution. It was vigorously stirred at 60 ℃ for 2 hours and was named Solution A. Subsequently, 3 min of nitric acid was added to 30 min of distilled water and vigorously stirred for 5 min, and it was named Solution B. Immediately after that, thiourea was added to 20 min of ethanol and thoroughly stirred for 5 min. Subsequently, 3 min of nitric acid was added and stirred at 60 ℃ for 1 hour, and it was named Solution C. Then, under the stirring state, Solution B and Solution C were poured into Solution A at intervals of 5 min successively. Finally, the obtained mixture was poured into the polytetrafluoroethylene liner in the autoclave and maintained at 100 ℃ for 24 hours. After centrifugal washing with ethanol, the sample was heated to 150 ℃ at a rate of 2 ℃/min and maintained at this temperature for 1 hour to remove the residual ethanol. After this stage was completed, the sample continued to be heated at the same rate until it reached 450 ℃ and was maintained at this temperature for 2 hours.

3.1.2. TiO_2 and $5\%N_{AB}/TiO_2$ Preparation

The preparation methods of $5\%N_{AB}/TiO_2$ and TiO_2 are the same as that of $5\%N_T/TiO_2$. The only difference is that the nitrogen precursor doped in $5\%N_{AB}/TiO_2$ is ammonium bicarbonate. And for TiO_2, no nitrogen precursor is added.

3.2. Catalyst Characterization

The crystalline structure and phase composition of TiO_2, $5\%N_T/TiO_2$ and $5\%N_T/TiO_2$ catalysts were determined by X-ray diffraction (XRD) method on an X-Pert diffractometer equipped with graphite monochromatized Cu-Kα radiation. The elemental composition, chemical states, and surface chemistry of TiO_2, $5\%N_T/TiO_2$ and $5\%N_T/TiO_2$ were analyzed using Agilent 5100 X-ray Photoelectron Spectroscopy (XPS), where tube voltage was 15kV, tube current was 10 mA and an ultra-high vacuum chamber with mu-metal magnetic shield was used. The specific surface areas were determined using a surface area analyzer (BEL Sorp-II mini, BEL Japan Co., Japan) with the Brunauer-Emmett-Teller (BET) method. The morphology and size of the TiO_2, $5\%N_T/TiO_2$ and $5\%N_T/TiO_2$ catalysts were observed using a Transmission Electron Microscope (TEM-16-TS-008). The acceleration voltage was 200 kV, the point resolution was 0.248 nm, and the maximum magnification was 1.05 million times to visualize the morphology, size, and surface features of TiO_2, $5\%N_T/TiO_2$ and $5\%N_T/TiO_2$ catalysts. The Fourier-Transform Infrared Spectroscopy (FTIR, Bruker Vertex 70 infrared

Preprints.org (www.preprints.org) | NOT PEER-REVIEWED | Posted: 22 August 2024 doi:10.20944/preprints202408.1629.v1

spectrometer) was used to analyze chemical bonds and functional groups present on the surface of TiO_2, 5%N_T/TiO_2 and 5%N_T/TiO_2 catalysts. FTIR spectra in transmission mode were recorded at a resolution of 4 cm^{-1} in the range of 400 to 1400 cm^{-1} using the KBr tabbing technique. The light absorption properties of TiO_2, 5%N_T/TiO_2 and 5%N_T/TiO_2 catalysts were determined by UV-Vis Spectroscopy with a wavelength range from 200 to 800 nm, on a Japanese Shimadzu UV-3600i Plus Spectrometer. The photocurrent and electrochemical impedance spectroscopy were measured on an electrochemical workstation.

3.3. Catalyst Evaluation

The performance of different catalysts in the photocatalytic degradation of MB is evaluated in a photocatalytic reactor under visible light irradiation. Firstly, 0.02 g catalyst was added to 20 mL MB. Adsorption and desorption equilibrium were attained by agitating the suspensions with a magnetic for 1 h. Afterward, the condensate water was turned on to keep the reaction temperature at room temperature. Then the solution was irradiated with an Xenon lamp as the source of visible light. An aliquot was collected periodically with a syringe from the reactor every 30 min during a 3 h interval. Finally, the catalyst was filtered and recycled. Changes in the concentration of MB were observed from its characteristic absorption at 664 nm using a UV-Vis spectrometer. The degradation efficiency of MB at each time point was calculated using the following formula[29,30]:

Degradation efficiency (%) = $\frac{Co-Ct}{Co} \times 100\%$

Where C_o is the initial concentration of MB and C_t is the concentration of MB at a time.

4. Conclusions

In conclusion, this work provides a straightforward method to fabricate nitrogen-doped TiO_2 photocatalysts based on thiourea as the N source. The systematic characterizations confirm the presence of nitrogen in TiO_2 crystalline. UV-vis spectra show the extended light absorption range on 5%N_T/TiO_2. Thus, 5%N_T/TiO_2 possesses better photocurrent response during PEC measurement. Through optimizing nitrogen concentration, 5%N_T/TiO_2 shows the highest MB degradation activity than TiO_2 and 5%N_{AB}/TiO_2 under visible light illumination. Our study clarifies the advantages of interstitial N doping in improving photocatalytic activity under visible light conditions. More importantly, this work demonstrates the introduction of nitrogen facilitates the utilization of solar light energy and leads TiO_2 to be a promising material for environmental remediation and beyond.

Author Contributions: D.L.: software, data curation, writing—review and editing. V.C.C.: validation, writing—original draft preparation. Y.L.: validation, visualization. H.L.: supervision, writing—review and funding. Y.L.: conceptualization, supervision and editing.

Funding: This work received financial support from the Young Talent Plan of Liaoning Province (XLYC2203068), Scientific Research Foundation of Technology Department of Liaoning Province of China (2022-MS-379) and National Natural Science Foundation of China (21902116).

Data Availability Statement: The data presented in this study are available on request from the corresponding author.

Acknowledgments: The program of China Scholarships Council (No. 202206250016) is acknowledged.

Conflicts of Interest: The authors declare no conflicts of interest.

Appendix A

X%N_T/TiO_2: where "x%" represents the doping amount of N; "T" represents that the selected N source is thiourea. X% N_{AB}/TiO_2: where "x%" represents the doping amount of N; "AB" represents that the selected N source is ammonium bicarbonate.

References

1. Sadek, O.; Touhtouh, S.; Dahbi, A.; Hajjaji, A. Photocatalytic Degradation of Methylene Blue on Multilayer TiO_2 Coatings Elaborated by the Sol-Gel Spin-Coating Method. *Water. Air. Soil Pollut.* **2023**, *234*, 698.

Preprints.org (www.preprints.org) | NOT PEER-REVIEWED | Posted: 22 August 2024 doi:10.20944/preprints202408.1629.v1

2. Ma, J.; Tian, Z.; Li, L.; Lu, Y.; Xu, X.; Hou, J. Loading Nano-CuO on TiO_2 Nanomeshes towards Efficient Photodegradation of Methylene Blue. *Catalysts* **2022**, *12*, 383.
3. Ma, Y.; Tao, L.; Bai, S.; Hu, A. Green Synthesis of Ag Nanoparticles for Plasmon-Assisted Photocatalytic Degradation of Methylene Blue. *Catalysts* **2021**, *11*, 1499.
4. Hariharalakshmanan, R.K.; Watanabe, F.; Karabacak, T. In Situ Growth and UV Photocatalytic Effect of ZnO Nanostructures on a Zn Plate Immersed in Methylene Blue. *Catalysts* **2022**, *12*, 1657.
5. Al-Ghouti, M.A.; Dib, S.S. Utilization of Nano-Olive Stones in Environmental Remediation of Methylene Blue from Water. *J. Environ. Heal. Sci. Eng.* **2020**, *18*, 63–77.
6. Haq, F.; Kiran, M.; Chinnam, S.; Farid, A.; Khan, R.U.; Ullah, G.; Aljuwayid, A.M.; Habila, M.A.; Mubashir, M. Synthesis of Bioinspired Sorbent and Their Exploitation for Methylene Blue Remediation. *Chemosphere* **2023**, *321*, 138000.
7. Xu, Y.; Shi, X.; Hua, R.; Zhang, R.; Yao, Y.; Zhao, B.; Liu, T.; Zheng, J.; Lu, G. Remarkably Catalytic Activity in Reduction of 4-Nitrophenol and Methylene Blue by Fe_3O_4@COF Supported Noble Metal Nanoparticles. *Appl. Catal. B Environ.* **2020**, *260*, 118142.
8. Malato, S.; Fernández-Ibáñez, P.; Maldonado, M.I.; Blanco, J.; Gernjak, W. Decontamination and Disinfection of Water by Solar Photocatalysis: Recent Overview and Trends. *Catal. Today* **2009**, *147*, 1–59.
9. Bairamis, F.; Konstantinou, I.; Petrakis, D.; Vaimakis, T. Enhanced Performance of Electrospun Nanofibrous TiO_2/g-C_3N_4 Photocatalyst in Photocatalytic Degradation of Methylene Blue. *Catal.* **2019**, *9*, 880.
10. Babyszko, A.; Wanag, A.; Sadłowski, M.; Kusiak-Nejman, E.; Morawski, A.W. Synthesis and Characterization of SiO_2/TiO_2 as Photocatalyst on Methylene Blue Degradation. *Catal.* **2022**, *12*, 1372.
11. Zhang, C.; Zhou, Y.; Bao, J.; Sheng, X.; Fang, J.; Zhao, S.; Zhang, Y.; Chen, W. Hierarchical Honeycomb Br-, N-Codoped TiO_2 with Enhanced Visible-Light Photocatalytic H_2 Production. *ACS Appl. Mater. Interfaces* **2018**, *10*, 18796–18804.
12. Assayehegn, E.; Solaiappan, A.; Chebude, Y.; Alemayehu, E. Fabrication of Tunable Anatase/Rutile Heterojunction N/TiO_2 Nanophotocatalyst for Enhanced Visible Light Degradation Activity. *Appl. Surf. Sci.* **2020**, *515*, 145966.
13. Chakraborty, A.K.; Ganguli, S.; Sabur, M.A. Nitrogen Doped Titanium Dioxide (N-TiO_2): Electronic Band Structure, Visible Light Harvesting and Photocatalytic Applications. *J. Water Process Eng.* **2023**, *55*, 104183.
14. Bissinger, D.; Honerkamp, J.H.; Roldan, J.; Bremes, J.; Kannen, K.; Lake, M.K.; Roppertz, A. Development of Catalytically Functionalized Polyester-Based Filters Produced by Flame Spray Pyrolysis. *Top. Catal.* **2024**, *67*, 539–550.
15. Khan, T.T.; Rafiqul Bari, G.A.K.M.; Kang, H.J.; Lee, T.G.; Park, J.W.; Hwang, H.J.; Hossain, S.M.; Mun, J.S.; Suzuki, N.; Fujishima, A.; et al. Synthesis of N-Doped TiO_2 for Efficient Photocatalytic Degradation of Atmospheric NOx. *Catal.* **2021**, *11*, 109.
16. Zhang, X.; Zuo, G.; Lu, X.; Tang, C.; Cao, S.; Yu, M. Anatase TiO_2 Sheet-Assisted Synthesis of Ti^{3+} Self-Doped Mixed Phase TiO_2 Sheet with Superior Visible-Light Photocatalytic Performance: Roles of Anatase TiO_2 Sheet. *J. Colloid Interface Sci.* **2017**, *490*, 774–782.
17. Sathish, M.; Viswanathan, B.; Viswanath, R. Alternate Synthetic Strategy for the Preparation of CdS Nanoparticles and Its Exploitation for Water Splitting. *Int. J. Hydrogen Energy* **2006**, *31*, 891–898.
18. Chen, X.; Burda, C. Photoelectron Spectroscopic Investigation of Nitrogen-Doped Titania Nanoparticles. *J. Phys. Chem. B* **2004**, 108, 15446–15449.
19. Pustovalova, A.A.; Pichugin, V.F.; Ivanova, N.M.; Bruns, M. Structural Features of N-Containing Titanium Dioxide Thin Films Deposited by Magnetron Sputtering. *Thin Solid Films* **2017**, *627*, 9-16.
20. Ren, W.; Ai, Z.; Jia, F.; Zhang, L.; Fan, X.; Zou, Z. Low Temperature Preparation and Visible Light Photocatalytic Activity of Mesoporous Carbon-Doped Crystalline TiO_2. *Appl. Catal. B Environ. Energy* **2007**, *69*, 138-144.
21. Di Valentin, C.; Pacchioni, G.; Selloni, A.; Livraghi, S.; Giamello, E. Characterization of Paramagnetic Species in N-Doped TiO_2 Powders by EPR Spectroscopy and DFT Calculations. *J. Phys. Chem. B* **2005**, *109*, 11414–11419.
22. Jiang, Z.-Y.; Ran, M.-J.; Liu, K.; Huang, Y.-F.; Li, Z.-R.; Shen, T.-T.; Li, W.-Y.; Khojiev, S.; Hu, Z.-Y.; Liu, J. Directing Ni/Al Layered Double Hydroxides Nanosheets on Tubular Graphite Carbon Nitride for Promoted Photocatalytic Hydrogen Production. *Mater. Today Chem.* **2024**, *39*, 102135.
23. Jiang, L.; Yu, H.; Shi, L.; Zhao, Y.; Wang, Z.; Zhang, M.; Yuan, S. Optical Band Structure and Photogenerated Carriers Transfer Dynamics in FTO/TiO_2 Heterojunction Photocatalysts. *Appl. Catal. B Environ.* **2016**, *199*, 224–229.
24. Li, Y.; Lai, R.; Luo, X.; Liu, X.; Ding, T.; Lu, X.; Wu, K. On the Absence of a Phonon Bottleneck in Strongly Confined $CsPbBr_3$ Perovskite Nanocrystals. *Chem. Sci.* **2019**, *10*, 5983–5989.
25. Zhu, Y.; Cui, Q.; Chen, J.; Chen, F.; Shi, Z.; Zhao, X.; Xu, C. Inhomogeneous Trap-State-Mediated Ultrafast Photocarrier Dynamics in $CsPbBr_3$ Microplates. *ACS Appl. Mater. Interfaces* **2021**, *13*, 6820–6829.

Preprints.org (www.preprints.org) | NOT PEER-REVIEWED | Posted: 22 August 2024 doi:10.20944/preprints202408.1629.v1

26. Das, D.; Shyam, S. Reduced Work Function in Anatase (101) TiO_2 Films Self-Doped by O-Vacancy-Dependent Ti^{3+} Bonds Controlling the Photocatalytic Dye Degradation Performance. *Langmuir* **2024**, *40*, 10502–10517.
27. Divyasri, Y.V.; Lakshmana Reddy, N.; Lee, K.; Sakar, M.; Navakoteswara Rao, V.; Venkatramu, V.; Shankar, M.V.; Gangi Reddy, N.C. Optimization of N Doping in TiO_2 Nanotubes for the Enhanced Solar Light Mediated Photocatalytic H_2 Production and Dye Degradation. *Environ. Pollut.* **2020**, *269*, 116170.
28. Bhowmick, S.; Saini, C.P.; Santra, B.; Walczak, L.; Semisalova, A.; Gupta, M.; Kanjilal, A. Modulation of the Work Function of TiO_2 Nanotubes by Nitrogen Doping: Implications for the Photocatalytic Degradation of Dyes. *ACS Appl. Nano Mater.* **2023**, *6*, 50–60.
29. Trandafilović, L. V; Jovanović, D.J.; Zhang, X.; Ptasińska, S.; Dramićanin, M.D. Enhanced Photocatalytic Degradation of Methylene Blue and Methyl Orange by ZnO: Eu Nanoparticles. *Appl. Catal. B Environ.* **2017**, *203*, 740–752.
30. Girotto, G.Z.; S. Thill, A.; Matte, L.P.; Vogt, M.A.H.; Machado, T. V; P. Dick, L.F.; Mesquita, F.; Bernardi, F. Ni/$SrTiO_3$ Nanoparticles for Photodegradation of Methylene Blue. *ACS Appl. Nano Mater.* **2022**, *5*, 13295–13307.

Disclaimer/Publisher's Note: The statements, opinions and data contained in all publications are solely those of the individual author(s) and contributor(s) and not of MDPI and/or the editor(s). MDPI and/or the editor(s) disclaim responsibility for any injury to people or property resulting from any ideas, methods, instructions or products referred to in the content.